Physica B 600 (2021) 412639

Contents lists available at ScienceDirect

Physica B: Physics of Condensed Matter

journal homepage: http://www.elsevier.com/locate/physb

Adsorption of lead on the surfaces of pristine and B, Si and N-doped graphene

Navaratnarajah Kuganathan [a,b,*], Sripathmanathan Anurakavan [c], Poobalasingam Abiman [c], Poobalasuntharam Iyngaran [c], Evangelos I. Gkanas [b], Alexander Chroneos [a,b]

[a] Department of Materials, Imperial College London, London, SW7 2AZ, United Kingdom
[b] Faculty of Engineering, Environment and Computing, Coventry University, Priory Street, Coventry, CV1 5FB, United Kingdom
[c] Department of Chemistry, University of Jaffna, Sir. Pon Ramanathan Road, Thirunelvely, Jaffna, Sri Lanka

ARTICLE INFO

Keywords:
Graphene
Binding energy
Doping
Lead adsorption
DFT

ABSTRACT

The efficacy of graphene and graphene doped with B, Si and N surfaces for the removal of Pb atom is examined by utilising density functional theory calculations. The results show that the binding energy of a single Pb atom on pristine graphene surface is −0.71 eV with the charge transfer of 0.42 electros from Pb to the surface. There is a significant enhancement observed in the binding on the surfaces of B-doped graphene (−1.46 eV) and Si-doped graphene (−2.37 eV) with the transfer of 1.48 and 1.92 electrons to their respective surfaces. The binding energy for the N-doped graphene is endothermic (+0.42 eV) due to negligible charge transfer between the Pb and the doped surface. The intense binding nature between Pb and pristine as well as the doped graphene structures is introduced, analysed and discussed in terms of bond distances, binding energies, Bader charges and electronic structures.

1. Introduction

Rapid human activities such as mining, smelting, electroplating and battery manufacturing produce a large volume of non-degradable heavy metals [1–4]. These toxic heavy metals have negative environmental impact, as they contaminate and pollute air, water and soil causing serious environmental and health problems. Lead (Pb) is one of the heavy metals mainly released from mining, paint and lead acid battery industries [5–7]. Its high degree of toxicity mainly affects the nervous system and kidneys with potential damage with overexposure [8–10]. Furthermore, at high concentrations, it can cause permanent disabilities such as learning difficulties, hearing loss, depression and anti-social behaviour [11,12].

Safe and efficient removal of lead is necessary, as there is a risk to human health when the concentrations of these metals are exceeded acceptable levels. In order to reduce its hazard, several techniques such as adsorption [13], solvent extraction [14], chemical precipitation [15], ion-exchange [16] and membrane filtration [17] have been used. Adsorption is one of the most promising technologies as this method is simple, efficient, cost effective and eco-friendly [18,19]. A variety of adsorbents including carbon nanotubes [20], minerals [21], activated carbon [22] and metal oxides [23] have been studied. A promising adsorbent should possess high thermal stability, high chemical stability, high surface area, high mechanical properties and less toxic.

Carbon nanomaterials such as carbon nanotubes, fullerenes, graphene and its derivatives have been recently attracted interest as promising adsorbents, mainly because of their large surface area, high mechanical strength, high flexibility and light weight [24–28]. Graphene is a two-dimensional lattice structure, with one-atom thick carbon atoms arranged on a honeycomb pattern. Due to these extraordinary thermal, mechanical and electrical properties, graphene has been considered as potential candidate for various applications. Graphene and its derivatives such as graphene oxides have been effectively utilised as adsorbents to remove lead ions from aqueous solutions [18,29,30]. Modification of graphene by doping p-type and n-type atoms is another way of increasing its adsorption capability. Many experimental and theoretical studies have considered the adsorption of atoms and molecules on the surfaces of doped carbon nanomaterials [31–37]. Furthermore, using quantum mechanical calculations it has been shown that dual-doped graphene dramatically increases the adsorption efficacy of Na and K [38,39]. The stability and electronic structure of triple-doped graphene has been discussed by Ullah et al. [40] and it is expected that

* Corresponding author. Department of Materials, Imperial College London, London, SW7 2AZ, United Kingdom.
E-mail addresses: n.kuganathan@imperial.ac.uk, ad0636@coventry.ac.uk (N. Kuganathan).

https://doi.org/10.1016/j.physb.2020.412639
Received 28 April 2020; Received in revised form 3 September 2020; Accepted 13 October 2020
Available online 14 October 2020

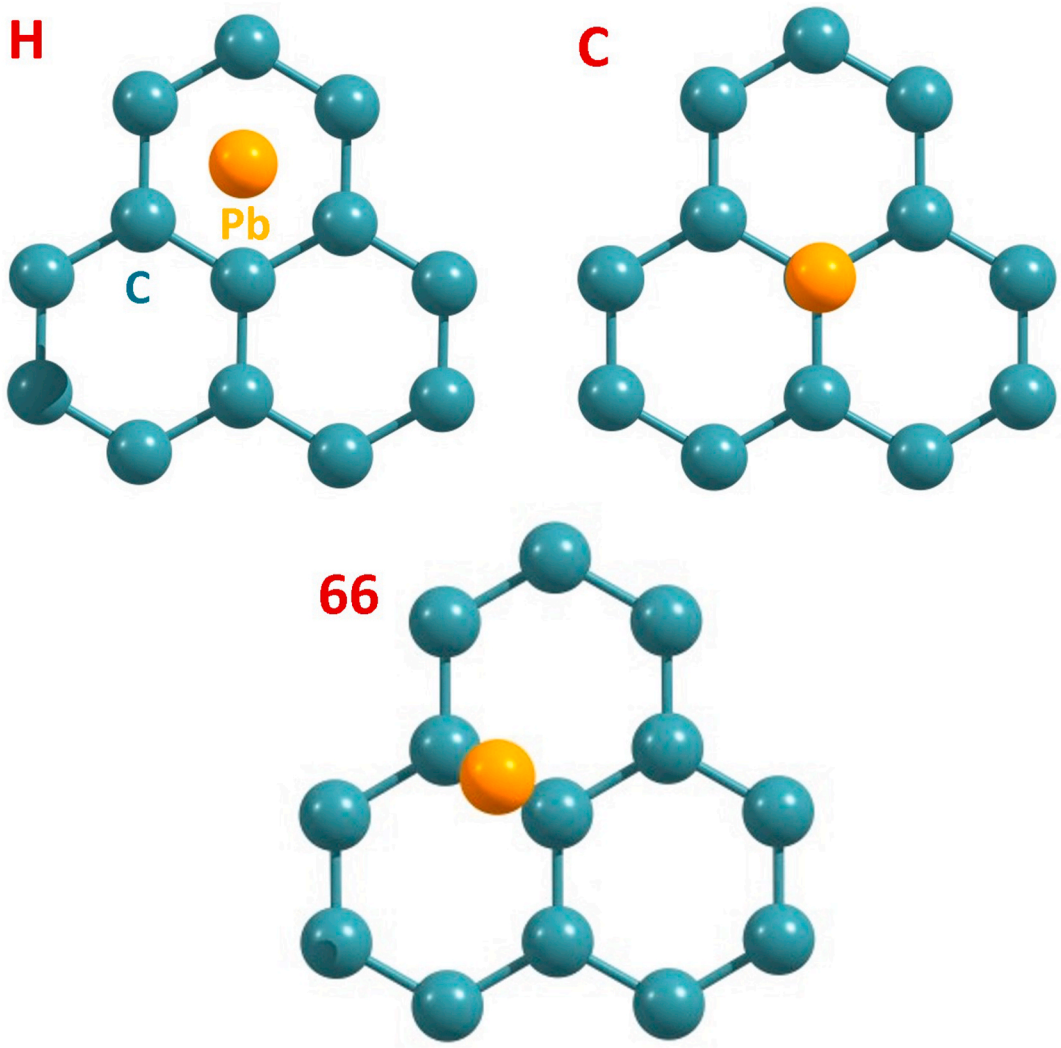

Fig. 1. Initial configurations of a single Pb atom adsorbed on the pristine graphene.

Table 1
Initial and final configurations of a single Pb atom adsorbed on different sites of graphene, adsorption energies, shortest Pb–C distances and the Bader charges on Pb atoms in the relaxed configurations.

Initial configuration	Final configuration	Adsorption energy (eV)	Pb–C (Å)	Bader charge on Pb (|e|)
H	H	–0.57	3.12	+0.40
C	C	–0.70	2.76	+0.39
66	**66**	–0.71	2.82	+0.42

there will be an enhancement in the adsorption of single atoms.

In this study, we use density functional theory (DFT) together with dispersion correction to examine the adsorption capability of Pb atom on the surfaces of pristine and B, Si and N-doped graphene in terms of bond distances, binding energies, Bader charges and electronic structures.

2. Computational methods

All calculations were performed using the plane wave DFT code VASP (Vienna Ab initio Simulation Package) [41] which uses plane wave basis sets and projected augment wave (PAW) pseudo-potentials [42]. In all calculations, a plane wave basis set with a cut-off of 500 eV and a 4 × 2 × 4 Monk-horst Pack [43] *k*-point mesh were used. The generalized gradient approximation (GGA) as parameterized by Perdew, Burke and Ernzerhof (PBE) [44] was applied to treat exchange-correlation effects. In order to minimize the energy of all geometries, conjugate gradient (CG) [45] algorithm was used. Forces on the atoms were less than 0.001 eV/Å in all optimized configurations. Dispersive attractive interactions were modelled using a DFT + D3 method parameterized by Grimme et al. [46].

We used a supercell consisting of 144 atoms within a cell dimension of $a = 25.0$ Å, $b = 15.0$ Å, $c = 30.0$ Å to make sure that the defects do not interact each other. The binding energy of a Pb atom in the gas phase adsorbed on pristine graphene was calculated using the following equation:

$$E_{bind} = E_{(Pb@Graphene)} - E_{(Graphene)} - E_{(Pb)} \quad (1)$$

where $E_{(Pb@Graphene)}$ is the total energy of a single Pb atom when adsorbed on the surface of graphene, $E_{(Graphene)}$ is the total energy of graphene and $E_{(Pb)}$ is the energy of an isolated gas phase Pb atom.

Substitution energy for a single boron atom to replace a single C atom on the graphene was calculated using the following equation:

$$E_{Sub} = E_{(B:Graphene)} + E_{(C)} - E_{(Graphene)} - E_{(B)}, \quad (2)$$

where $E_{(B:Graphene)}$ is the total energy of a single B atom doped on the surface of graphene, $E_{(Graphene)}$ is the total energy of graphene and $E_{(C)}$ and $E_{(B)}$ are the energies of isolated gas phase C and B atoms respectively.

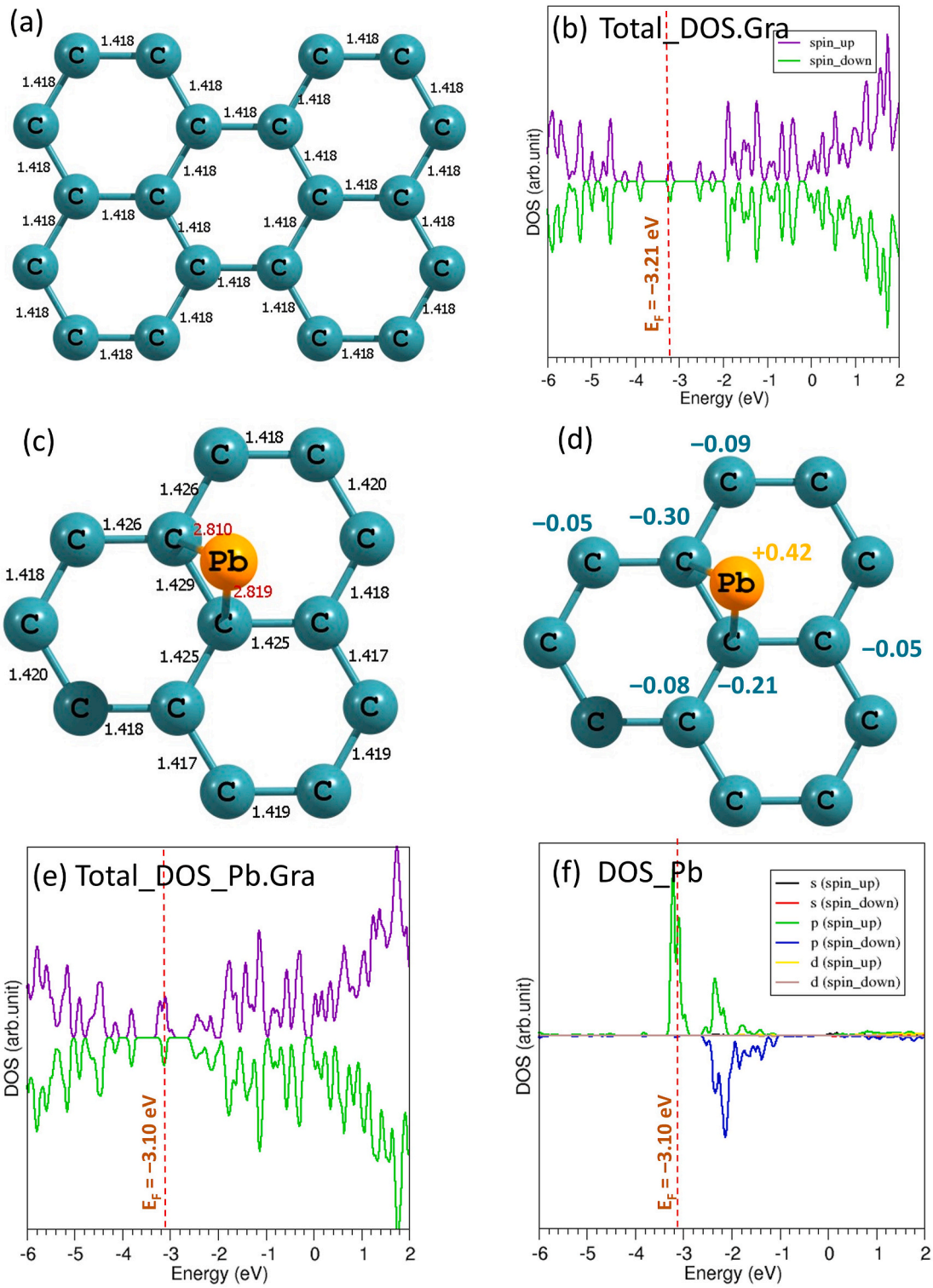

Fig. 2. **(a)** Relaxed structure of graphene, (b) total DOS plot of graphene (c) relaxed structure of a Pb atom adsorbed on the bridge site (66) (d) total DOS plot of Pb atoms adsorbed on graphene and (e) atomic DOS plot of Pb.

Binding energy of a gas phase Pb atom adsorbed on a boron-doped graphene was calculated using the following equation:

$$E_{bind} = E_{(Pb@B:Graphene)} - E_{(B:Graphene)} - E_{(Pb)} \quad (3)$$

where $E_{(Pb@B:Graphene)}$ is the total energy of a single Pb atom adsorbed on the surface of B-doped graphene, $E_{(B:Graphene)}$ is the total energy of B-doped graphene and $E_{(Pb)}$ is the energy of an isolated gas phase Pb atom.

Lead atom will be in the form of Pb^{2+} in aquatic environments. In some cases (e.g. during mining and vehicle emission), Pb atom will be in the form of gases or particulates. In such cases, calculations using Pb atom as reference state are adequate enough. However, the choice of Pb^{2+} as reference state can be of interest in a situation where Pb atom is present in an environmental solution. In this case, interaction between Pb^{2+} ions in adjacent cells should be eliminated by considering supercells with large dimension.

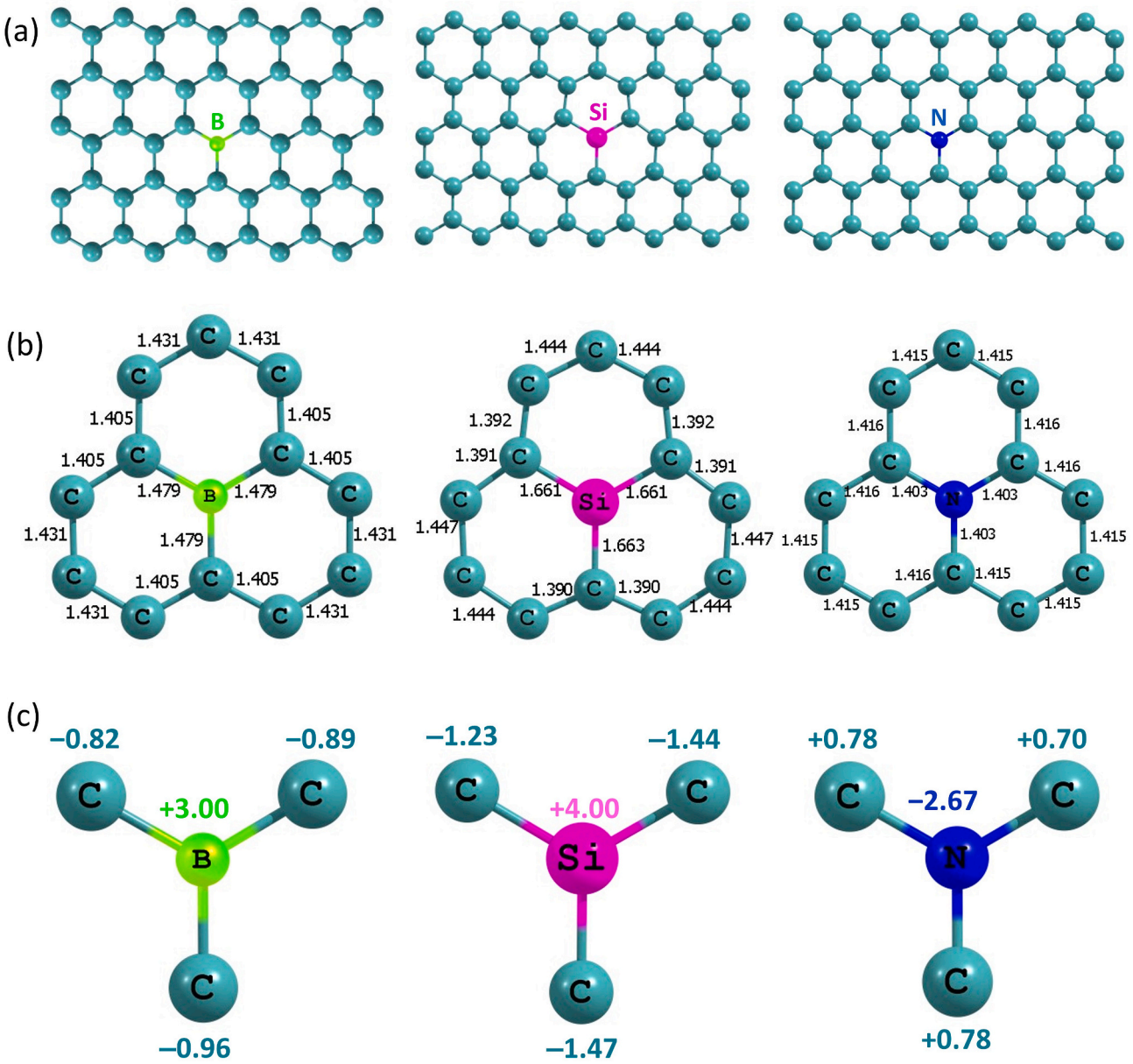

Fig. 3. (a) Relaxed configurations of B, Si and N doped graphene, (b) bond distances around the doped atoms and (c) Bader charges on the doped atoms and C atoms attached to them.

Table 2
Substitution energies (calculated using the metal atom as the reference state), electro negativities of doped atoms, shortest X–C bond distances (X = B, Si and N) and the Bader charges on the doped atoms.

X in X•Graphene (X = B, Si and N)	Electronegativity [48]	Substitution energy (eV)	X–C (Å)	Bader charge on X (|e|)
B	1.91	2.42	1.48	+3.00
Si	1.82	8.18	1.66	+4.00
N	3.01	3.29	1.40	−2.97

3. Results and discussion

3.1. Adsorption of Pb atom on the surface of pristine graphene

First we considered the adsorption of a single Pb atom on the surface of graphene. Three possible initial adsorption sites were identified as illustrated in Fig. 1. Top of the center hexagonal ring is denoted as "**H**". The "**66**" site means that Pb atom resides on top of a C–C bond between two hexagonal rings. The site in which Pb atom resides on top of a C atom is defined as "**C**".

In Table 1 we report the final configurations, binding energies, shortest Pb–C bond distances, and the Bader charges on Pb atoms. Fig. 2 shows the relaxed structures of pristine graphene showing C–C bond distances, total density of states (DOS) of graphene, relaxed structure of Pb atom adsorbed on the 66 site, Bader charges on the Pb atom and its adjacent C atoms, total DOS plot and atomic DOS plot of Pb. In all the studied cases, the initial and the final configurations are the same. The **66** site is identified as the most favourable adsorption site with the binding energy of −0.71 eV. The difference in the binding energy between 66 and C is only 0.01eV. The binding energy for the site H is 0.14 eV lower than that calculated for 66 site. This is reflected in the longer Pb–C bond distance (Table 1). In all cases, the binding energies are negative; thus, the pristine graphene would trap Pb atom without energy cost. The Bader charge analysis [47] shows that there is a small charge

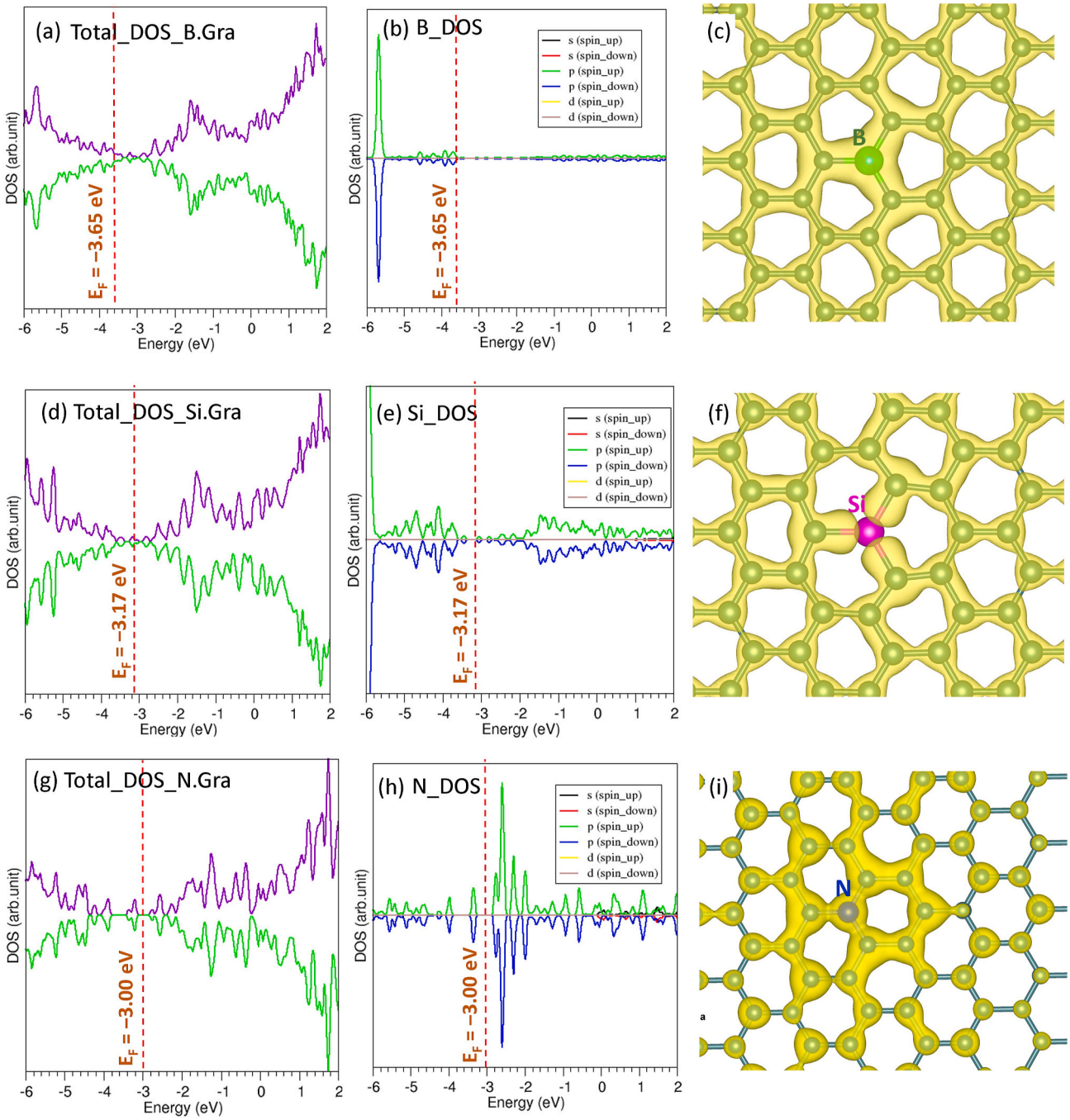

Fig. 4. (a) Total DOS plot of B-doped graphene, (b) atomic DOS plot of B and (c) constant charge density plot associated with the B atom and its neighbour C atoms. Similar plots are shown for Si (d–f) and N (g–i).

transfer (~0.40 *e*) from Pb to the graphene surface. This is related to the higher electronegativity of C (2.52) as compared with the Pb (1.56) [48]. The electrons transferred from the Pb are mainly localised on the bridge C atoms (Fig. 2d). Adsorption introduces a small elongation (0.09 Å) in the bridge C–C bond distance (Fig. 2c). The C–C bond distance in a pristine graphene is reported to be 1.42 Å which is in good agreement with the outcomes of the present study (Fig. 2a) [49]. The DOS plot calculated in this study is in agreement with other theoretical studies [49,50]. Adsorption shifts the Fermi energy level to the conduction band by 0.11 eV. Atomic DOS plotted for Pb confirms that electronic states around the Fermi energy mainly from the Pb (refer to Fig. 2e).

3.2. Doping of graphene with B, Si and N

In order to enhance the degree of binding, the graphene surface was modified by doping with B (electron-acceptor), Si (isovalent) and N (electron-donor) atoms. Fig. 3 shows the optimized structures of doped graphene. Calculated substitution energy of B is 2.42 eV (Table 2). This indicates that the C–C bond is stronger than the B–C bond as evidenced by the shorter C–C bond length. In the pristine graphene, the C–C bond length is calculated to be 1.418 Å (Fig. 2a). The B–C bond length is 0.06 Å longer than the C–C bond length in the pristine graphene (Fig. 3b). Also there is a small perturbation noted in the C–C bond lengths slightly further away from the dopants. The Bader charge analysis shows that the B donates its three outer electrons to the adjacent three C atoms (Fig. 3c)

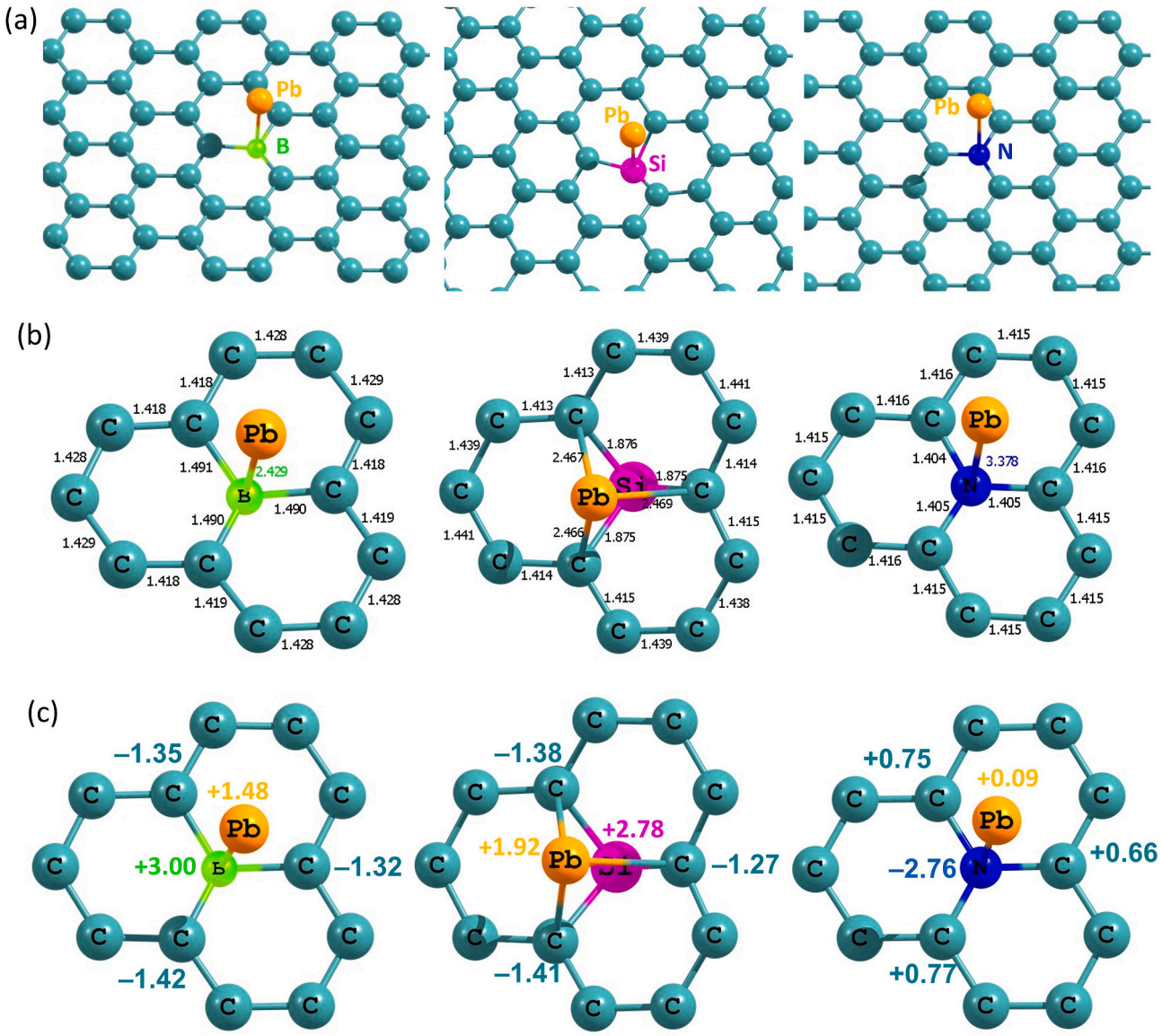

Fig. 5. (a) Relaxed configurations of Pb adsorbed on the surfaces of B, Si and N doped graphene, (b) bond distances around the doped atoms and (c) Bader charges on the doped atoms, the Pb and the C atoms attached to them.

Table 3
Adsorption energies (calculated using the Pb atom as the reference state), shortest X–C/X–Pb bond distances (X = B, Si and N) and Bader charges on the doped atoms and Pb.

X in Pb@X•Graphene (X = B, Si and N)	Adsorption energy (eV)	X–C (Å)	X–Pb (Å)	Bader charge (|e|)	
				X	Pb
B	−1.46	1.49	2.43	+3.00	+1.48
Si	−2.37	1.88	3.02	+2.78	+1.92
N	+0.42	1.41	3.38	−2.76	+0.09

inferring the higher electronegativity of C (2.52) than B (1.92) [48]. Doping of B shifts the Fermi level to the valence bands by 0.55 eV (Fig. 4a). The states associated with the B appear near the Fermi level and at ~−6 eV (refer to Fig. 4b). Fig. 4c confirms the electron distribution around the B and its nearest neighbour C atoms as observed in the Bader charge analysis.

In the case of Si doping, the substitution energy is calculated to be 8.18 eV higher by ~6 eV than that calculated for B. This is reflected in the significant distortion around the Si and the hexagonal rings. The Si–C bonds are longer by ~0.25 Å than the C–C bonds (refer to Fig. 4b). The Bader charge on the Si is +4.00. This means that the Si has donated its four outer electrons to the nearest neighbour C atoms as evidenced by the negative charge localised on the C atoms according to the Bader charge (refer to Fig. 3c). It is also noted that the electronegativity of C (2.52) is higher than that of Si (1.82) [48]. A very small shift in the Fermi energy level is observed (refer to Fig. 4d). The states arising from the Si lies between −3.50 eV and −6.00 eV. The constant charge density plot showing the charge distribution around the Si is shown in Fig. 4f.

Doping of N is exothermic as noted for the other two dopants and its substitution energy is 3.29 eV. The distortion is observed to be small. The C–N bond distances are longer than only 0.02 Å compared to C–C bonds in the pristine graphene (refer to Fig. 3b). In contrast to previous two cases, charge transfer is observed from C atoms to the N. This is due to the higher electronegativity of N (3.01) than that of C (2.52) [48]. The N prefers to form complete outer electronic configuration of s^2p^6 according to the Bader charge in which N has gained ~3 electrons from adjacent three C atoms making them positively charged (refer to

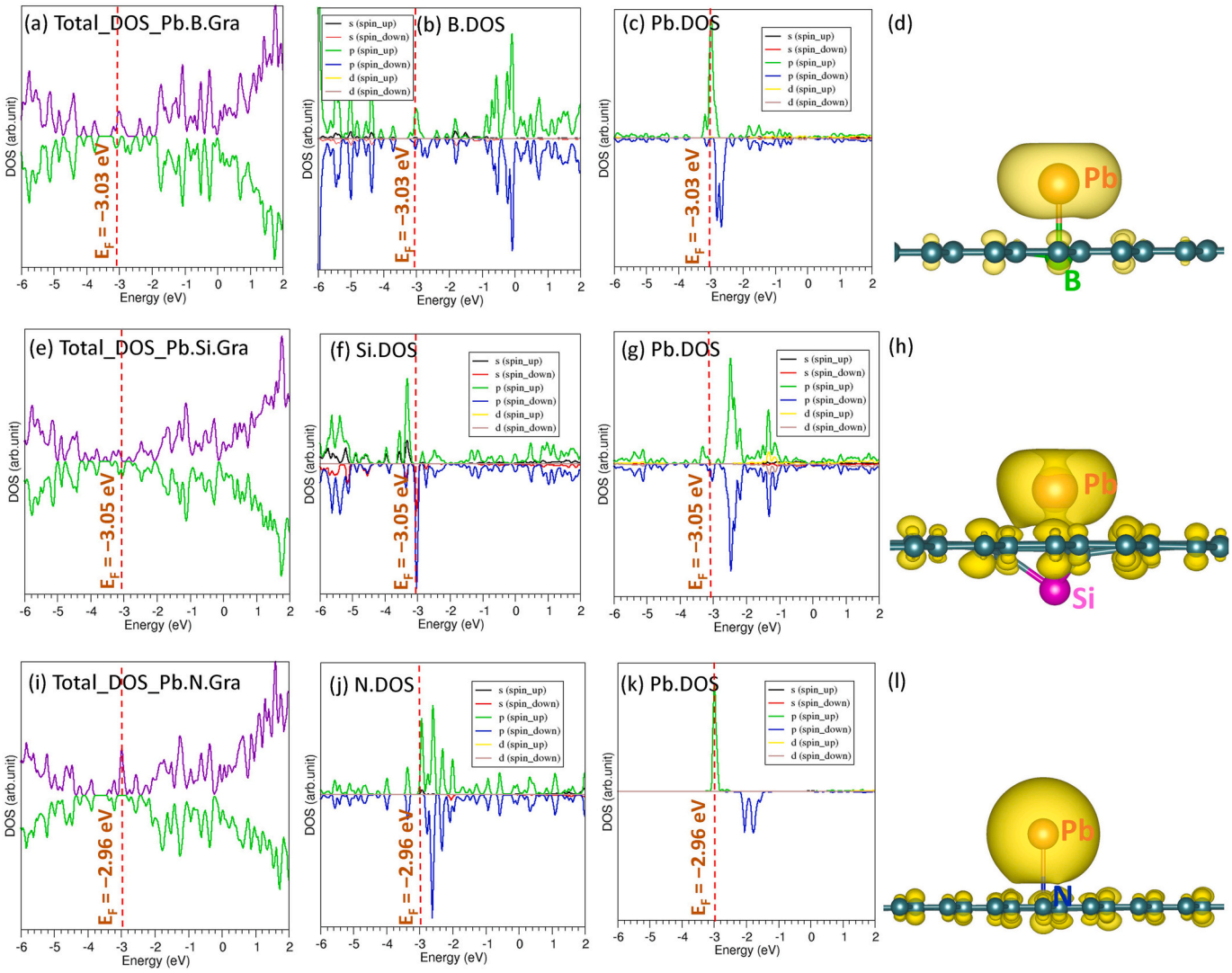

Fig. 6. (a) Total DOS plot calculate for the B-doped graphene, (b) atomic DOS plot of B (c) atomic DOS plot of Pb and (d) constant charge density plot associated with the Pb and its neighbour C atoms. Similar plots are shown for Si (e–h) and N (i–l).

Fig. 3c). A small reduction in the Fermi energy is noted for the N–doped graphene compared to that of pristine graphene. The states associated with the N are scattered between −3.20 eV and −6.00 eV.

3.3. Adsorption of Pb atom on the surface of doping graphene

Finally, the doped surface structures were considered for the adsorption of Pb atom. The relaxed structures are shown in Fig. 5. For the case of doping with B, exoergic adsorption energy (−1.46 eV) was calculated (Table 3). The adsorption potentiality is almost doubled as compared to the case of the pristine graphene. This behaviour is related to the significant charge transfer (1.48 *e*) from Pb to the surface as compared to the charge transfer from Pb to the pristine graphene surface. This is further evidenced by high negative charges on the C atoms attached to the B (Fig. 5c). The Pb–C bond distance is calculated to be 2.429 Å (Fig. 5b). The B–C bond distances are slightly elongated compared to those calculated in the absence of Pb. Calculated the DOS plot shows that there is a reduction in the Fermi energy by 0.62 eV compared to that calculated for B-doped graphene (Fig. 6). The additional states appear near the Fermi energy are mainly from *p* states of Pb. Significant enhancement in the adsorption of Pb is observed for the Si-doped graphene. This is due to the increment in the donation of electrons from the Pb to the surface and reduction in the charge on the Si. The Bader charge analysis shows that Pb and Si atoms donate 1.92 and 2.78 electrons respectively to the surface. Both the Pb and the Si atoms form trigonal pyramid configurations (refer to Fig. 5b). There is a small shift observed in the Fermi energy compared to that calculated for both pristine graphene and Si-doped graphene.

The adsorption energy calculated for the N-doped surface is endoergic (0.42 eV) meaning that there is no binding between the Pb atom and the surface. This is further confirmed by the negligible charge transfer between the Pb to the surface, longer Pb–N distance of 3.378 Å and almost the same Bader charges on the N-doped graphene (refer to Fig. 5). The DOS plots show that the states appearing near the Fermi level is mainly from the Pb. The Fermi energy (−2.96 eV) is almost the same compared to that calculated for N-doped graphene (−3.00 eV) and differs only by 0.25 eV with that calculated for pristine graphene.

4. Conclusions

In the present study, we have investigated the binding nature of a Pb atom on pristine and doped-graphene surfaces using density functional theory calculations together with dispersion correction. The lowest substitution energy has been obtained for B. It is found that B and Si doped-graphene structures enhance the binding as compared to the case of the pristine graphene surface. This is related to the significant charge

transfer. The N-doped graphene is not suitable for the adsorption Pb atoms, as it exhibits an endoergic binding energy and a very small charge transfer. We anticipate that this theoretical prediction can stimulate experiments to validate and apply these materials for adsorbing Pb atoms.

Credit author contribution statement

Navaratnarajah Kuganathan: Investigation, Data curation, Writing - original draft. Sripathmanathan Anurakavan: Formal analysis. Poobalasingam Abiman: Formal analysis. Poobalasuntharam Iyngaran: Formal analysis. Evangelos I. Gkanas: Writing - review & editing. Alexander Chroneos: Writing - review & editing.

Funding

The author(s) received no financial support for the research.

Declaration of competing interest

The authors declare that they have no known competing financial interests or personal relationships that could have appeared to influence the work reported in this paper.

Acknowledgments

We acknowledge Coventry University and Imperial College London for providing computational facilities.

References

[1] M. Tsezos, Biosorption of metals. The experience accumulated and the outlook for technology development, Hydrometallurgy 59 (2001) 241–243.
[2] C.M. Park, J. Han, K.H. Chu, Y.A.J. Al-Hamadani, N. Her, J. Heo, Y. Yoon, Influence of solution pH, ionic strength, and humic acid on cadmium adsorption onto activated biochar: experiment and modeling, J. Ind. Eng. Chem. 48 (2017) 186–193.
[3] K.H. Vardhan, P.S. Kumar, R.C. Panda, A review on heavy metal pollution, toxicity and remedial measures: current trends and future perspectives, J. Mol. Liq. 290 (2019) 111197.
[4] J. Cook, Environmental pollution by heavy metals, Int. J. Environ. Stud. 10 (1977) 253–266.
[5] G. Liu, Y. Yu, J. Hou, W. Xue, X. Liu, Y. Liu, W. Wang, A. Alsaedi, T. Hayat, Z. Liu, An ecological risk assessment of heavy metal pollution of the agricultural ecosystem near a lead-acid battery factory, Ecol. Indicat. 47 (2014) 210–218.
[6] H.F. Clark, D.J. Brabander, R.M. Erdil, Sources, sinks, and exposure pathways of lead in urban garden soil, J. Environ. Qual. 35 (2006) 2066–2074.
[7] M.A.S. Laidlaw, G.M. Filippelli, Resuspension of urban soils as a persistent source of lead poisoning in children: a review and new directions, Appl. Geochem. 23 (2008) 2021–2039.
[8] A.L. Wani, A. Ara, J.A. Usmani, Lead toxicity: a review, Interdiscipl. Toxicol. 8 (2015) 55–64.
[9] T.W. Clarkson, Metal toxicity in the central nervous system, Environ. Health Perspect. 75 (1987) 59–64.
[10] L.H. Mason, J.P. Harp, D.Y. Han, Pb neurotoxicity: neuropsychological effects of lead toxicity, BioMed Res. Int. (2014) (2014) 840547-840547.
[11] S. Jamesdaniel, R. Rosati, J. Westrick, D.M. Ruden, Chronic lead exposure induces cochlear oxidative stress and potentiates noise-induced hearing loss, Toxicol. Lett. 292 (2018) 175–180.
[12] J.W. Reyes, Lead exposure and behaviour: effects on antisocial and risky behaviour among children and adolescents, Econ. Inq. 53 (2015) 1580–1605.
[13] Z. Mahdi, Q.J. Yu, A. El Hanandeh, Removal of lead(II) from aqueous solution using date seed-derived biochar: batch and column studies, Applied Water Science 8 (2018) 181.
[14] M. Černá, Use of solvent extraction for the removal of heavy metals from liquid wastes, Environ. Monit. Assess. 34 (1995) 151–162.
[15] D. Kavak, Removal of lead from aqueous solutions by precipitation: statistical analysis and modeling, Desalination and Water Treatment 51 (2013) 1720–1726.
[16] A. Lalmi, K.-E. Bouhidel, B. Sahraoui, C.e.H. Anfif, Removal of lead from polluted waters using ion exchange resin with $Ca(NO_3)_2$ for elution, Hydrometallurgy 178 (2018) 287–293.
[17] K.C. Khulbe, T. Matsuura, Removal of heavy metals and pollutants by membrane adsorption techniques, Applied Water Science 8 (2018) 19.
[18] M. Kumar, S.J. Chung, H.S. Hur, Graphene composites for lead ions removal from aqueous solutions, Appl. Sci. 9 (2019).
[19] Renu, M. Agarwal, K. Singh, Heavy metal removal from wastewater using various adsorbents: a review, Journal of Water Reuse and Desalination 7 (2016) 387–419.
[20] X. Ren, C. Chen, M. Nagatsu, X. Wang, Carbon nanotubes as adsorbents in environmental pollution management: a review, Chem. Eng. J. 170 (2011) 395–410.
[21] W.-R. Lim, S.W. Kim, C.-H. Lee, E.-K. Choi, M.H. Oh, S.N. Seo, H.-J. Park, S.-Y. Hamm, Performance of composite mineral adsorbents for removing Cu, Cd, and Pb ions from polluted water, Sci. Rep. 9 (2019) 13598.
[22] A.J. Ahamed, V. Balakrishnan, Studies on the adsorption of ferrous ion from aqueous solution by low cost carbon, J. Chem. Pharmaceut. Res. 2 (2010) 733–745.
[23] F. A M. Salem, R. T, M. Ossman, Metal oxide nano-particles as an adsorbent for removal of heavy metals, J. Adv. Chem. Eng. 5 (2015).
[24] N. Selvanantharajah, P. Iyngaran, P. Abiman, Quantitative studies of cadmium ion (Cd2+) adsorption on oxidized graphite powder, Mater. Today: Proceedings 23 (2020) 105–110.
[25] B.-M. Jun, S. Kim, Y. Kim, N. Her, J. Heo, J. Han, M. Jang, C.M. Park, Y. Yoon, Comprehensive evaluation on removal of lead by graphene oxide and metal organic framework, Chemosphere 231 (2019) 82–92.
[26] L. Xu, J. Wang, The application of graphene-based materials for the removal of heavy metals and radionuclides from water and wastewater, Crit. Rev. Environ. Sci. Technol. 47 (2017) 1042–1105.
[27] S. Mallakpour, E. Khadem, 8 - carbon nanotubes for heavy metals removal, in: G. Z. Kyzas, A.C. Mitropoulos (Eds.), Composite Nanoadsorbents, Elsevier, 2019, pp. 181–210.
[28] E. Ciotta, P. Prosposito, P. Tagliatesta, C. Lorecchio, L. Stella, S. Kaciulis, P. Soltani, E. Placidi, R. Pizzoferrato, Discriminating between different heavy metal ions with fullerene-derived nanoparticles, Sensors 18 (2018) 1496.
[29] S. Mohan, V. Kumar, D.K. Singh, S.H. Hasan, Effective removal of lead ions using graphene oxide-MgO nanohybrid from aqueous solution: isotherm, kinetic and thermodynamic modeling of adsorption, Journal of Environmental Chemical Engineering 5 (2017) 2259–2273.
[30] M. Khazaei, S. Nasseri, M.R. Ganjali, M. Khoobi, R. Nabizadeh, E. Gholibegloo, S. Nazmara, Selective removal of lead ions from aqueous solutions using 1,8-dihydroxyanthraquinone (DHAQ) functionalized graphene oxide; isotherm, kinetic and thermodynamic studies, RSC Adv. 8 (2018) 5685–5694.
[31] W. Wang, Y. Zhang, C. Shen, Y. Chai, Adsorption of CO molecules on doped graphene: a first-principles study, AIP Adv. 6 (2016), 025317.
[32] N. Kuganathan, N. Selvanantharajah, P. Iyngaran, P. Abiman, A. Chroneos, Cadmium trapping by C60 and B-, Si-, and N-doped C_{60}, J. Appl. Phys. 125 (2019), 054302.
[33] Y. Wang, J. Chen, X. Huang, Adsorption behavior of B-doped/N-doped graphene sheets toward NO2, NO and NH3 molecules: a first-principles study, Phys. Status Solidi C 14 (2017) 1600110.
[34] J. Wang, Y. Chen, L. Yuan, M. Zhang, C. Zhang, Scandium decoration of boron doped porous graphene for high-capacity hydrogen storage, Molecules 24 (2019) 2382.
[35] P.A. Denis, Band gap opening of monolayer and bilayer graphene doped with aluminium, silicon, phosphorus, and sulfur, Chem. Phys. Lett. 492 (2010) 251–257.
[36] P.A. Denis, When noncovalent interactions are stronger than covalent bonds: bilayer graphene doped with second row atoms, aluminum, silicon, phosphorus and sulfur, Chem. Phys. Lett. 508 (2011) 95–101.
[37] P.A. Denis, Chemical reactivity and band-gap opening of graphene doped with gallium, germanium, arsenic, and selenium atoms, ChemPhysChem 15 (2014) 3994–4000.
[38] P.A. Denis, Lithium adsorption on heteroatom mono and dual doped graphene, Chem. Phys. Lett. 672 (2017) 70–79.
[39] S. Ullah, P.A. Denis, F. Sato, Unusual enhancement of the adsorption energies of sodium and potassium in Sulfur−Nitrogen and Silicon−Boron codoped graphene, ACS Omega 3 (2018) 15821–15828.
[40] S. Ullah, P.A. Denis, F. Sato, Triple-doped monolayer graphene with boron, nitrogen, aluminum, silicon, phosphorus, and sulfur, ChemPhysChem 18 (2017) 1864–1873.
[41] G. Kresse, J. Furthmüller, Efficient iterative schemes for ab initio total-energy calculations using a plane-wave basis set, Phys. Rev. B 54 (1996) 11169–11186.
[42] P.E. Blöchl, Projector augmented-wave method, Phys. Rev. B 50 (1994) 17953–17979.
[43] H.J. Monkhorst, J.D. Pack, Special points for Brillouin-zone integrations, Phys. Rev. B 13 (1976) 5188–5192.
[44] J.P. Perdew, K. Burke, M. Ernzerhof, Generalized gradient approximation made simple, Phys. Rev. Lett. 77 (1996) 3865–3868.
[45] W.H. Press, S.A. Teukolsky, W.T. Vetterling, B.P. Flannery, Numerical Recipes in C (2nd ed.): the Art of Scientific Computing, Cambridge University Press, 1992.
[46] S. Grimme, J. Antony, S. Ehrlich, H. Krieg, A consistent and accurate ab initio parametrization of density functional dispersion correction (DFT-D) for the 94 elements H-Pu, J. Chem. Phys. 132 (2010) 154104.
[47] W. Tang, E. Sanville, G. Henkelman, A grid-based Bader analysis algorithm without lattice bias, J. Phys. Condens. Matter 21 (2009), 084204.
[48] W. Gordy, W.J.O. Thomas, Electronegativities of the elements, J. Chem. Phys. 24 (1956) 439–444.
[49] H. Gao, Z. Liu, DFT study of NO adsorption on pristine graphene, RSC Adv. 7 (2017) 13082–13091.
[50] M. Yang, C. Zhang, S. Wang, Y. Feng, Ariando, Graphene on β-Si_3N_4: an ideal system for graphene-based electronics, AIP Adv. 1 (2011), 032111.